I.J. Wireless and Microwave Technologies, **2023, 3, 49-63**
Published Online on June 8, 2023 by MECS Press (http://www.mecs-press.org/)
DOI: 10.5815/ijwmt.2023.03.05

Performance Evaluation of Slotted Star-Shaped Dual-band Patch Antenna for Satellite Communication and 5G Services

Md. Najmul Hossain*
Department of Electrical, Electronic and Communication Engineering, Pabna University of Science and Technology, Pabna-6600, Bangladesh
E-mail: najmul_eece@pust.ac.bd
ORCID iD: https://orcid.org/0000-0002-2528-9168
*Corresponding Author

Al Amin Islam
Department of Electrical, Electronic and Communication Engineering, Pabna University of Science and Technology, Pabna-6600, Bangladesh
E-mail: alaminislam8150@gmail.com
ORCID iD: https://orcid.org/0000-0002-4230-2176

Jungpil Shin
School of Computer Science and Engineering, The University of Aizu, Aizuwakamatsu, Fukushima 965-8580, Japan
E-mail: jpshin@u-aizu.ac.jp
ORCID iD: https://orcid.org/0000-0002-7476-2468

Md. Abdur Rahim
Department of Computer Science and Engineering, Pabna University of Science and Technology, Pabna-6600, Bangladesh
E-mail: rahim@pust.ac.bd
ORCID iD: https://orcid.org/0000-0003-2300-1420

Md. Humaun Kabir
Department of Computer Science and Engineering, Faculty of Engineering, Bangamata Sheikh Fojilatunnesa Mujib Science & Technology University, Jamalpur-2012, Bangladesh
E-mail: humaun@bsfmstu.ac.bd
ORCID iD: https://orcid.org/0000-0001-7225-0736

Received: 01 October, 2022; Revised: 23 November, 2022; Accepted: 24 December, 2022; Published: 08 June, 2023

Abstract: The advancement of wireless communication technology is growing very fast. For next-generation communication systems (like 5G mobile services), wider bandwidth, high gain, and small-size antennas are very much needed. Moreover, it is expected that the next-generation mobile system will also support satellite technology. Therefore, this paper proposes a slotted star-shaped dual-band patch antenna that can be used for the integrated services of satellite communication and 5G mobile services whose overall dimension is $15\times14\times1.6$ mm^3. The proposed antenna operates from 18.764 GHz to 19.775 GHz for K-band satellite communication and 27.122 GHz to 29.283 GHz for 5G (mmWave) mobile services. The resonance frequencies of the proposed antenna are 19.28 GHz and 28.07 GHz having bandwidths of 1.011 GHz and 2.161 GHz, respectively. Moreover, the proposed dual-band patch antenna has a maximum radiation efficiency of 76.178% and a maximum gain of 7.596 dB.

Index Terms: Dual-band Patch Antenna, mmWave, Satellite Communication, 5G Mobile Services.

1. Introduction

The swift technological development in telecommunications, including radar, satellite technology, and mobile phones, is remarkable. Dual-band antennas can operate on two different frequency bands simultaneously, whereas two single-band antennas must be used for the same operations. So, Dual-band antennas reduce the fabrication cost, the device's size, and the system's complexity. For this reason, there is a great demand for dual-band antennas in telecommunication networks [1, 2].

The next generation of mobile networks will be heterogeneous, flexible, and able to accommodate on-the-fly application requirements. As a result, it must be able to support service offerings on a much larger scale [3]. Due to the accelerating development of wireless and radio telecommunication systems, the consumer of wireless communication services will continue to increase daily. The number of connected devices will be exceeded 50 billion very soon. In this case, low-cost, less complex, higher data rates, and minimal data traffic systems will be needed. The current generation of wireless communication networks (4G) cannot fulfill these requirements because of many limitations. Therefore, the fifth-generation wireless communication network (5G) has become indispensable to meeting the above requirements. Designing a high-performing antenna (like miniatured size, higher data rates, higher radiation gain, etc.) in mmWave like 5G services is challenging. In this case, a patch antenna can be a convenient solution as these antennas have many advantages like miniature size, low cost, better gain, and an easy fabrication process [4-8]. Fig. 1 shows the networking scenarios based on different signal coverage areas in the mmWave bands.

The millimeter-wave (mmWave) bands provide new facilities with a massive quantity of spectrum to fifth-generation (5G) mobile communication networks to meet the rapidly growing demand for mobile data. In terms of directivity, susceptibility to obstruction, and high propagation loss, there are significant differences between traditional systems and mmWave communications. The much greater bandwidth of mmWave opens up many possibilities for a 5G cellular connection. The coverage of mmWave-based cellular networks is higher, and the capacity potential is higher [9]. With these requirements in mind, researchers have introduced antennas for 5G services and other mmWave applications using several techniques such as array structure, meta-material structure, slot structure, defected ground structure (DGS), and so on. For example, a rectangle patch dual-band antenna with a miniaturized size has been proposed in the paper [10]. It has a narrow operating bandwidth and gains 6.4 dBi and 5.4 dBi at 28 GHz and 37 GHz, respectively.

In this paper, we proposed a slotted star-shaped dual-band circular patch antenna that can be used for the integrated service of K-band satellite communication and 5G mobile services. The proposed antenna exhibits very good impedance matching over the frequency bands of 18.764 GHz to 19.775 GHz for K-band satellite communication and 27.122 GHz to 29.283 GHz for 5G (mmWave) mobile services, along with a minimum return loss of -28.31 dB at the operating frequency of 19.28 GHz. The characteristics of the proposed antenna, such as return loss, antenna gain, and radiation patterns, are investigated in this paper. The computer simulation technology microwave studio (CST-MWS) found all the simulation results. CST-MWS is a well-known and frequently used software for estimating an antenna system's radiation characteristics. Constructing, examining, and optimizing any electromagnetic system provides a comprehensive range of solvers and tools. The primary characteristics of the suggested dual-band circular patch antenna can be summarized as follows.

- The gain of the suggested antenna is comparatively higher; it is also small and able to operate at dual-band frequencies.
- At the relevant resonant frequencies, the suggested antenna's bandwidth is also greater than that of the standard patch antenna.
- The antenna will support higher data rates because it was made for 5G networks.
- The suggested antenna can be used for the integrated K-band satellite and 5G mobile communications services.

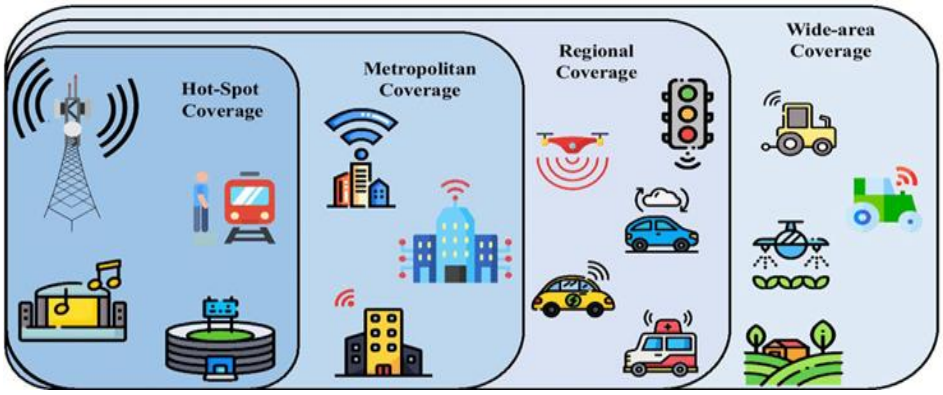

Fig. 1. Coverage scenarios for mmWave in 5G mobile networks and beyond [3]

The remainder of the paper is organized as follows. The following section presents the literature review. Section 3 describes the theory and model of the proposed slotted star-shaped dual-band circular patch antenna. Section 4 deals with the performance evaluation of the proposed antenna based on the simulation results. Section 5 provides a comparison of the performance of the proposed antenna to the recently published works. Finally, the conclusion of our manuscript is drawn in section 6.

2. Literature Review

A lot of research was done before the design of the proposed antenna. In [11], another dual-band mmWave patch antenna based on an array structure is presented with a complicated structure having a narrow bandwidth. The resonance frequencies are 24.9 GHz and 28 GHz, and the gains are 5.375 dB and 8.42 dB, respectively. In [12], a dual-band slotted patch antenna has been designed using a slot structure for mmWave wireless applications. It operates at 24.25 GHz and 38 GHz with a gain of 5.541 dB and 4.527 dB, respectively. Also, a miniature patch antenna has been introduced using the DGS technique in [13]. This antenna resonates with the 5G frequency band at 28 GHz and provides a gain of 7.6 dB, where the return loss value is - 56.95 dB.

Moreover, another small-sized patch antenna has been proposed using the Iterative Method in [14]. The proposed design resonates at 28 GHz and delivers a gain of 5.45 dB. Using the DGS technique, the antenna bandwidth has been improved from 1.2 GHz to 2 GHz. Furthermore, another dual-band microstrip patch antenna is presented in [15] for 5G mobile services. It has an impedance bandwidth of 1.90 GHz and 1.01 GHz at 24.16 GHz and 28.1 GHz frequency, respectively. Recently, researchers have also shown a great interest in designing such types of dual-band antennas that can be used for X-band (8 GHz to 12 GHz), Ku-band (12 GHz to 18 GHz), and K-band (18 GHz to 27 GHz) satellite communications [16-23]. Also, many designers are focusing on designing such types of dual-band or multiband antennas that can be used for the integrated service of WiMAX and military satellite or satellite, radar communications and 5G (mmWave) services or satellite communications, 5G (mmWave) mobile services and the other wireless applications [24-29].

3. Theory and Design Specification of the Proposed Patch Antenna

3.1 Theory

The width W and length L of any rectangular shape patch antenna are calculated with the help of the following equations [2].

$$W = \frac{c}{2f_0\sqrt{\frac{\varepsilon_r+1}{2}}} \tag{1}$$

Where f_0 is the resonant frequency and ε_r is the dielectric constant. The radiations pass through the air and some through the substrate to reach the ground. The air and the substrate have different dielectric constant values; therefore, an effective dielectric constant (ε_{eff}) has to be considered, which is calculated using the given equation [10].

$$\varepsilon_{eff} = \frac{\varepsilon_r+1}{2} + \frac{\varepsilon_r-1}{2}\left[1+\frac{12h}{W}\right]^{-1/2} \tag{2}$$

Where h is the thickness of the substrate. The length of the patch is calculated using equation [10].

$$L = \frac{c}{2f_0\sqrt{\varepsilon_{eff}}} \tag{3}$$

Electrically the size of the antenna is increased by an amount of ΔL due to fringing. The increased length is given by using equation (4).

$$\Delta L = 0.412h\,\frac{(\varepsilon_{eff}+0.3)(\frac{W}{h}+0.264)}{(\varepsilon_{eff}-0.258)(\frac{W}{h}+0.8)} \tag{4}$$

The minimum length (L_{sub}) and width (W_{sub}) of the substrate are calculated using equations (5) and (6).

$$L_{sub} = 6h + L \tag{5}$$

$$W_{sub} = 6h + W \tag{6}$$

Now, the circular patch design consists of calculating the radius (R) and the inset feed length (F) and is given by [14]

$$R = \frac{F}{\left[1+\frac{2h}{\pi\varepsilon_r F}\left(ln\left(\frac{\pi F}{2h}\right)+1.7729\right)^{1/2}\right.} \tag{7}$$

Where F= $\frac{8.791\times10^9}{f_r\sqrt{\varepsilon_r}}$. The above equations obtain the radius of the circular patch shape.

3.2 Design Specification of the Proposed Patch Antenna

The geometrical structure of the proposed slotted star-shaped circular patch antenna is shown in Fig. 2, where the overall dimension of the antenna is 15×14×1.6 mm^3. The proposed design and simulation have been carried out using CST-MWS2017 software. The proposed dual-band antenna consists of a circular radiating patch with a star-shaped slot and two rectangular-shaped slots. These slots have been introduced to operate the antenna in the desired dual-band operation. The dimensions of both rectangular slots are the same. The slotted circular patch conductor is made of copper metal and has a radius (a) of 2.75 mm, whereas its thickness (t_p) is 0.018 mm. It is developed on the Rogers RT5880 (lossy) dielectric substrate with a dielectric permittivity of 2.2 and loss tangent of 0.0009, and copper material has also been used in the ground plane. The thickness of the substrate material (t_s) is 1.6 mm, where the thickness of the ground plane (t_g) and the patch conductor (t_p) are the same. The parameters used for the proposed dual-band slotted star-shaped patch antenna are shown in Table 1. To drive the antenna, a 50 Ω microstrip feedline is used. To get the proper impedance matching, the width of the feedline (g) has been chosen as 0.8 mm.

The evolutionary steps of antenna design to attain the desired dual-band operation for K-band satellite communication (19.28 GHz) and 5G mobile services (28.07 GHz) are shown in Fig. 3. The proposed design has been completed in four steps. Fig. 3(a) illustrates the 1st step, a conventional circular patch antenna. The initial patch antenna (step 1) resonates at 20.98 GHz and 31.117 GHz frequencies with a return loss of -15.10 dB and -11.16 dB. It operates from 20.319 GHz to 21.589 GHz, and 30.222 GHz to 33.022 GHz frequencies, respectively, where 2nd band is not applicable for mmWave 5G services and the return loss is high, as shown in Fig. 4(a). The return loss of the different steps of the antenna is discussed in detail in the simulation results section. Also, the radiation pattern is not well for the 2nd band, as shown in Fig. 7(b). To shift the resonating frequency for the 2nd band towards the mmWave (28 GHz) 5G communication and improve the antenna's performance, the initial patch is modified by inserting a star-shaped and rectangular slot.

In the 2nd step, a rectangular slot similar to the patch antenna structure [30] is introduced in the initial patch shown in Fig. 3(b). Due to the insertion of this rectangular slot, the resonating frequencies have shifted from right to left and improved return loss for both bands, shown in Fig. 4(b). The antenna resonates at 20.58 GHz and 29.899 GHz frequencies with a return loss of -25.594 dB and –14.139 dB, respectively. Also, it has increased antenna gain for the 2nd band, and the radiation pattern for the 1st band is better than step 1, which is shown in Fig. 7(d), Fig. 8(e), and Fig. 8(f), respectively.

In the 3rd step, a star-shaped slot is introduced on the patch to improve the antenna's performance. If an eight-point star-shaped slot similar to the structure of the patch antenna [31] had been used in step 3, it would have overlapped with the rectangular slot and a portion of the feedline, which will affect greatly changed the performance parameters (like antenna gain, radiation patterns, etc.) of the antenna. Also, the antenna will act as a single-band or ultra-width band patch antenna. But our work aims to design a high-performance dual-band patch antenna. For this reason, a five-point star-shaped slot is used in step 3 to improve the performance of the 1st modified antenna. Due to the insertion of this slot (step 3), the radiation pattern for the 2nd band has improved, which is much better than step 2, as shown in Fig. 7(f), Fig. 9(c), and Fig. 9(d), respectively. Also, Fig. 4(c) shows that it has increased bandwidth for the 2nd band, where the resonating frequencies have shifted from right to left.

Due to the insertion of the star-shaped slot on the patch (step 3), the return loss for the 1st band reached high, shown in Fig. 4(c). Therefore, another symmetrical rectangular slot (similar to step 2) is inserted on the patch to shift the resonating frequency and improve the return loss with other performance parameters of the antenna (step 4) is shown in Fig. 3(d) where the proposed design resonates at the 19.28 GHz and 28.07 GHz frequencies, respectively.

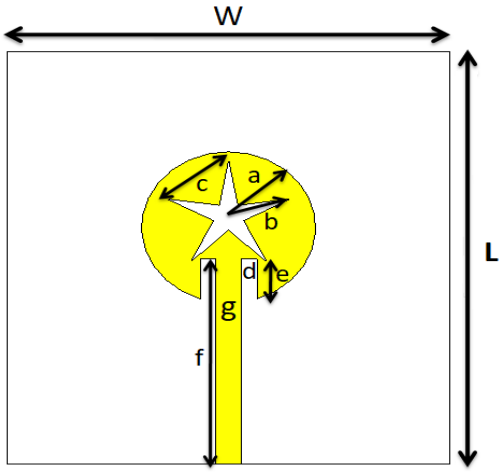

Fig. 2. The geometry of the proposed slotted star-shaped circular patch antenna

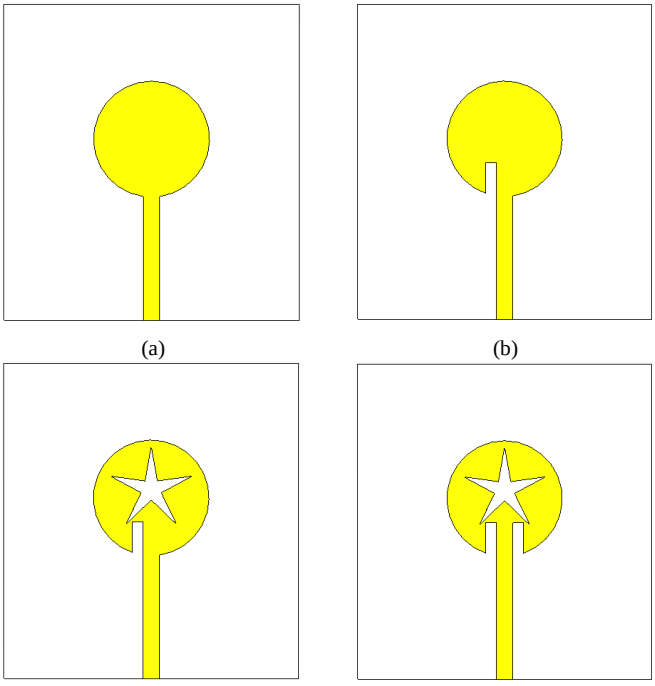

Fig. 3. Geometrical evolution for the proposed slotted star-shaped antenna (a): Step 1: Initial antenna, (b): Step 2: 1st modified antenna, (c): Step 3: 2nd modified antenna, (d): Step 4: Proposed antenna

Table 1. Dimension Details of the Proposed Antenna.

Parameters	**Values (mm)**
Length of substrate (L_s)	15
Length of the ground plane (L_g)	15
The thickness of the substrate (t_s)	1.6
The radius of the patch (a)	2.75
Distance between two points of the star (c)	1.35
Width of feed line (g)	0.8
Width of substrate (W_s)	14
Width of the ground plane (W_g)	14
The thickness of the ground plane and patch (t_g=t_p)	0.018
Distance from the center of the star to the vertex (b)	2
Width of the rectangular slot (d)	0.5
Length of feed line (f)	7.45
Length of the rectangular slot (e)	1.35

4. Performance Evaluation of the Proposed Antenna

A simulation has been performed using CST-MWS Studio 2017. The results are presented here for S-parameter (return loss), VSWR, surface currents, radiation patterns, radiation gain, directivity, and radiation efficiency.

4.1 S-Parameters

When the magnitude of the S-parameter (S_11) is expressed in decibels (dB), it is called return loss. The return loss can be expressed in terms of the reflection coefficient, Γ as:

$$RL(dB) = -20log|\Gamma| \tag{8}$$

For an antenna to radiate effectively, the return loss should be less than 10 dB.

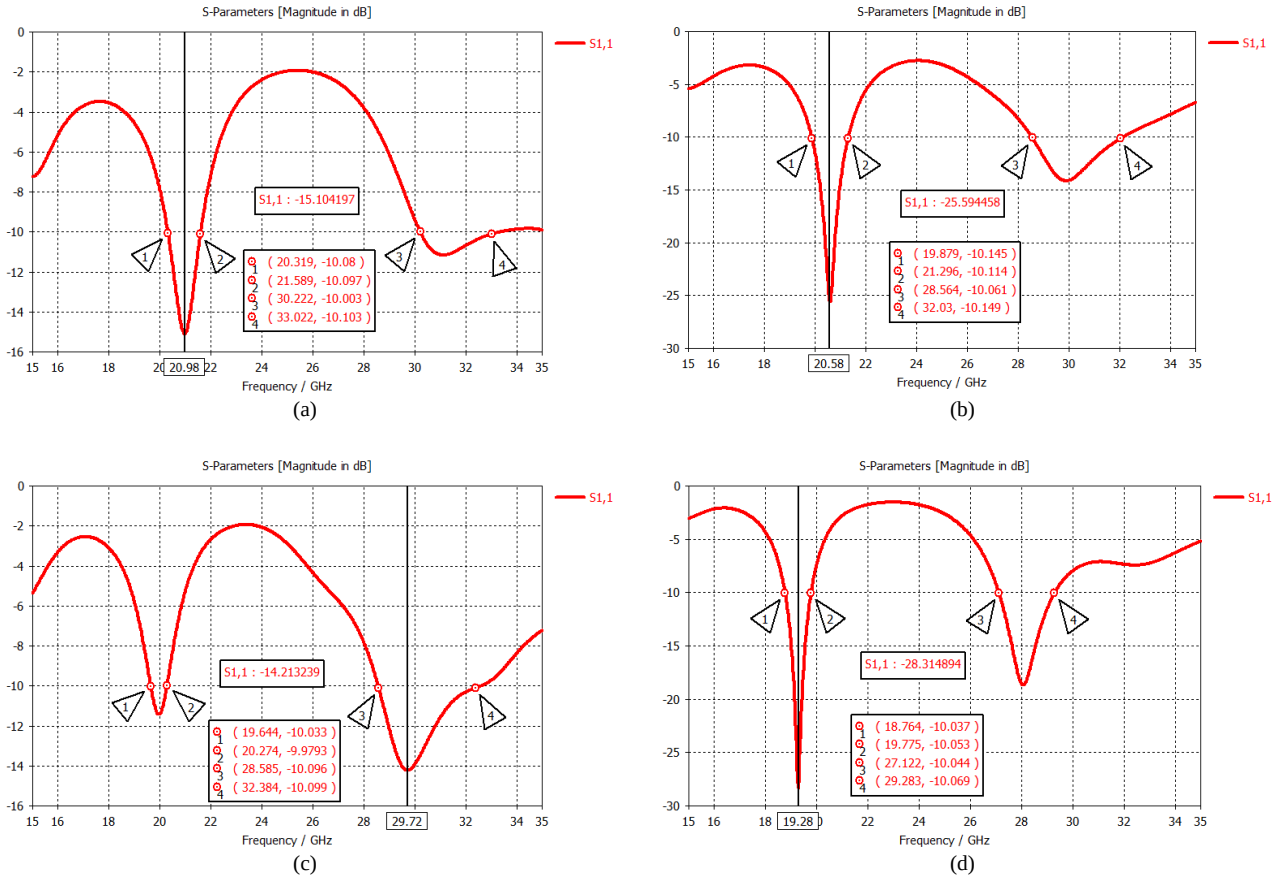

Fig. 4. Return loss curve of the circular and slotted star-shaped patch antenna (a): Initial, (b): 1st modified, (c): 2nd modified, (d): Proposed slotted star-shaped

Fig. 4(a) shows the return loss of the initial circular shape patch antenna (step 1). This antenna resonates at 20.98 GHz and 31.117 GHz frequencies with a return loss of -15.10 dB and -11.16 dB, respectively. The return loss curve of the 1st modified antenna (step 2) is shown in Fig. 4(b). From the curve, we see that it exhibits dual-band properties and works in two different frequency bands from 19.879 to 21.296 GHz and 28.564 to 32.03 GHz with corresponding bandwidths of 1.417 GHz and 3.466 GHz, respectively. It resonates at 20.58 GHz and 29.899 GHz frequencies with return losses of approximately -25.594 dB and –14.139 dB, respectively. Fig. 4(c) shows the return loss of the 2nd modified (step 3) antenna where the resonant frequencies have shifted. It resonates at 19.962 GHz and 29.72 GHz frequencies with return losses of –11.427 dB and –14.213 dB, respectively. This design works in two frequency bands, from 19.644 to 20.274 GHz and 28.585 to 32.384 GHz, respectively.

The return loss of the proposed slotted star-shaped patch antenna (step 4) is illustrated in Fig. 4(d), which defines and measures the resonance frequency and bandwidth of the antenna. This antenna has two desired operating frequency bands ranging from 18.764 to 19.775 GHz and 27.122 to 29.283 GHz, corresponding bandwidths of 1.011 GHz and 2.161 GHz, respectively. It resonates at 19.28 GHz and 28.07 GHz frequencies with return losses of approximately–28.314 dB and –18.662 dB, respectively. The 1st band is suitable for K-band satellite communication, whereas the 2nd band can be used for 5G (mmWave) mobile services.

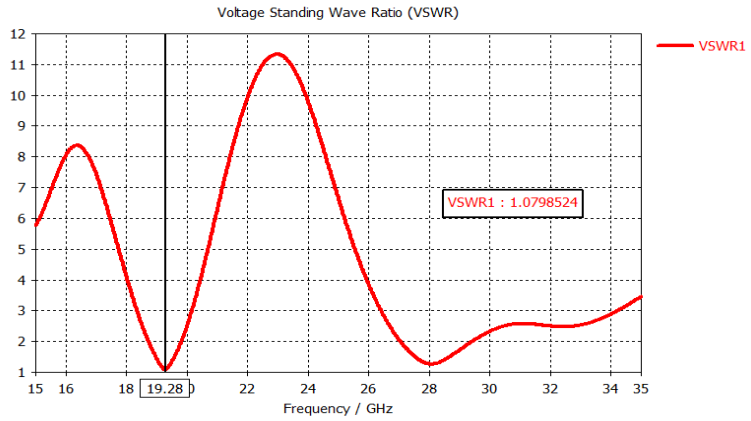

Fig. 5. VSWR curve of the proposed slotted star-shaped patch antenna

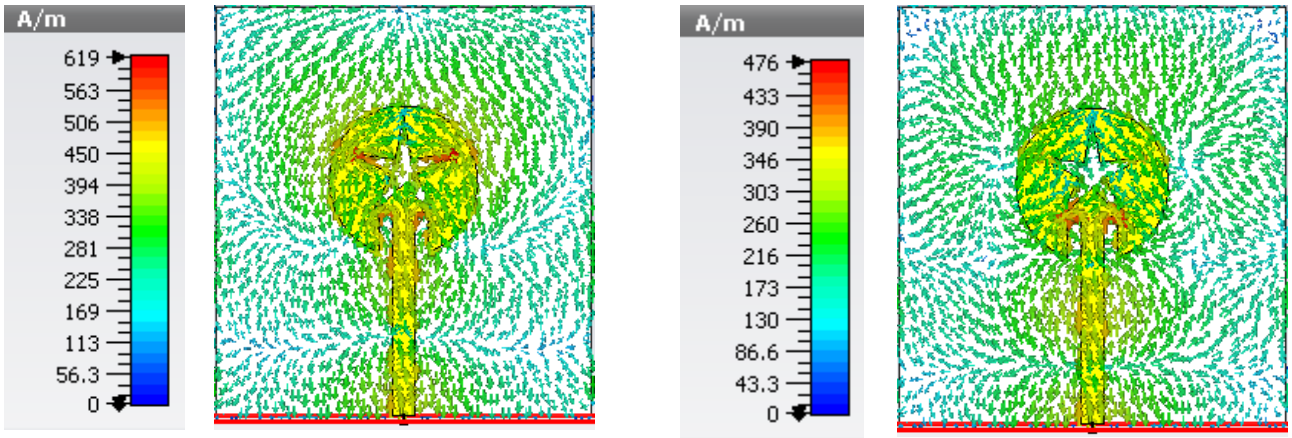

(a) (b)

Fig. 6. Surface current distributions of the proposed patch antenna (a): at 19.28 GHz, (b): at 28.07 GHz

4.2 Voltage Standing Wave Ratio (VSWR)

VSWR (Voltage Standing Wave Ratio) is a measure that describes the amount of mismatch between an antenna and the feeding system that connects to it. The VSWR is given by,

$$VSWR = \frac{1+|\Gamma|}{1-|\Gamma|} \tag{9}$$

Where Γ represents the reflection coefficient. The higher the VSWR, the greater the mismatch. A perfect impedance match is obtained when ZL (antenna's input impedance)$= ZO$ (the corresponding RF circuitry's output impedance), which gives the reflection coefficient Γ a value of zero, and the VSWR becomes unity which is the ideal condition. But practically, for antenna applications, its value should be less than 2. Fig. 5 explains the impedance matching of the proposed design, where it exhibits a VSWR value of 1.079 and 1.264 at the 19.28 GHz and 28.07 GHz resonance frequencies, respectively, representing a proper impedance matching for the antenna.

4.3 Surface Current Distribution

Surface currents illustrate how the current propagates over the radiating element in the antenna structure. Fig. 6(a) and 6(b) illustrate the surface current distribution of the proposed dual-band slotted star-shaped patch antenna. From Fig. 6(a), we see that at 19.28 GHz, a strong distribution of surface currents appears on the radiating patch and especially around the star slot. This star slot is responsible for making a 19.28 GHz K-band satellite communications band where the maximum value of the surface current is 618.9 A/m. Fig. 6(b) shows that at 28.07 GHz, the strongest surface currents have located in the upper part of both rectangular slots. These slots are responsible for creating the 28.07 GHz 5G (mmWave) mobile services band, where the value of surface current is 476.2 A/m.

4.4 Radiation Pattern, Gain, and Directivity

The radiation pattern describes how an antenna radiates energy or receives energy. Radiation gain indicates how strong an antenna can send or receive signals in a certain direction. Figs. 7(a) and 7(b) show the 3D gain radiation patterns for the initial patch antenna (step 1), respectively. The antenna gains are 8.507 dB and 6.502 dB at the resonating frequencies, but the radiation pattern is not well manner for the 2nd band where Figs. 7(c) and 7(d) show 3D

Gain patterns for the 1st modified antenna, respectively. It exhibits a gain of 8.295 dB and 7.387 dB at the resonance frequencies. Also, Fig. 7(e) and Fig. 7(f) exhibit the 3D Gain radiation patterns for the 2nd modified antenna (step 3), where the antenna gains are 8.098 dB and 6.644 dB at the 19.962 GHz and 29.72 GHz resonance frequencies, respectively, and radiation patterns for the 2nd band is much better than the step 2.

The simulated 3D Gain radiation patterns of the proposed dual-band slotted star-shaped patch antenna at 19.28 GHz and 28.07 GHz frequencies are illustrated in Fig. 7(g) and Fig. 7(h), respectively. It has been seen that the values of radiation gain of the proposed antenna at 19.28 GHz and 28.07 GHz frequencies are 7.596 dB and 6.972 dB, respectively.

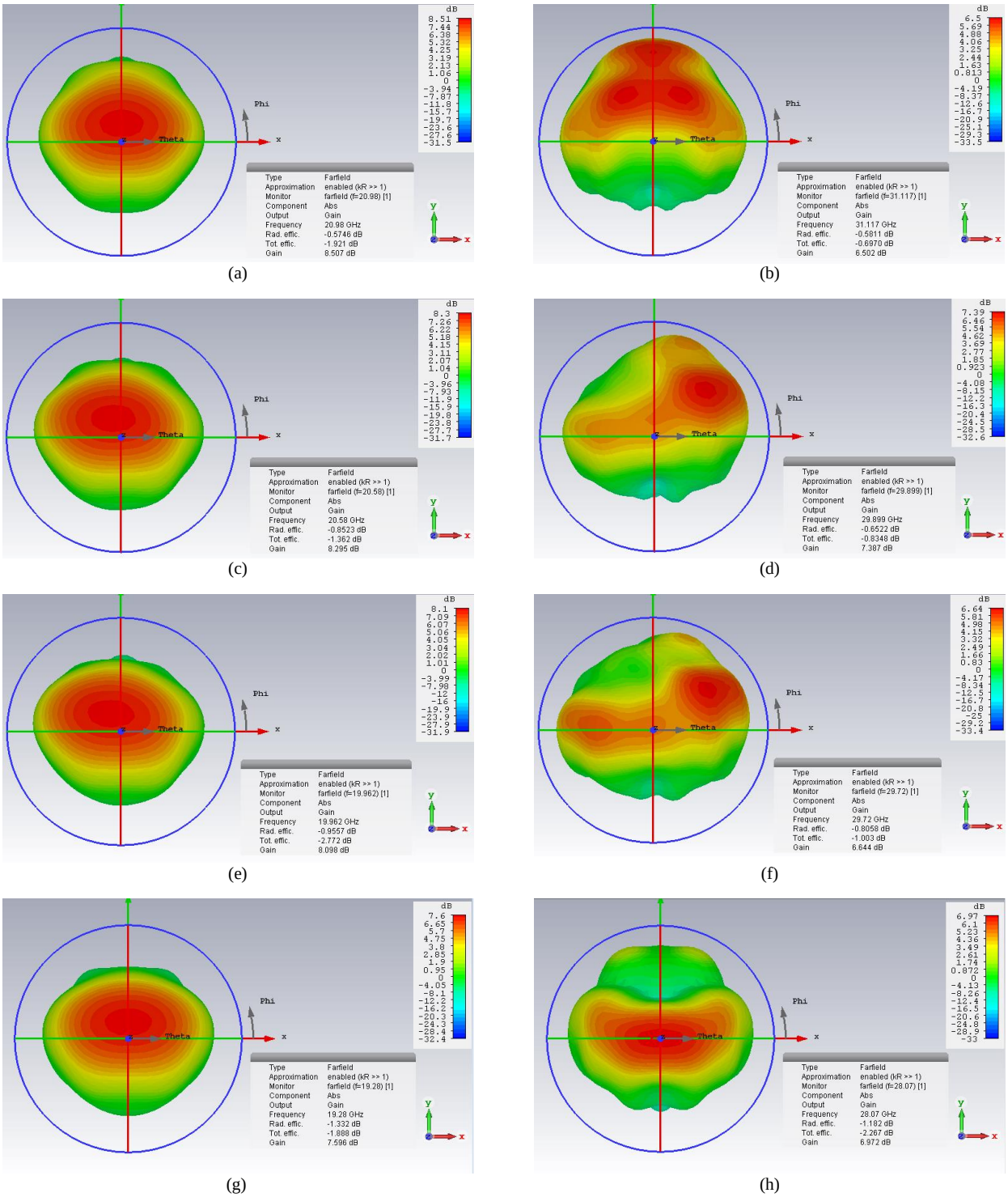

Fig. 7. 3D Gain radiation patterns (a): at 20.98 GHz, (b): at 31.117 GHz, (c): at 20.58 GHz, (d): at 29.899 GHz, (e): at 19.962 GHz, (f): at 29.72 GHz, (g): at 19.28 GHz, (h): at 28.07 GHz

The simulated Farfield radiations patterns of the initial patch antenna (step 1) for E-plane (XZ-plane, phi=0 °) and H-plane (XY-plane, phi=90 °) at 20.98 GHz and 31.117 GHz resonance frequencies are shown in Fig. 8(a) to Fig. 8(d).

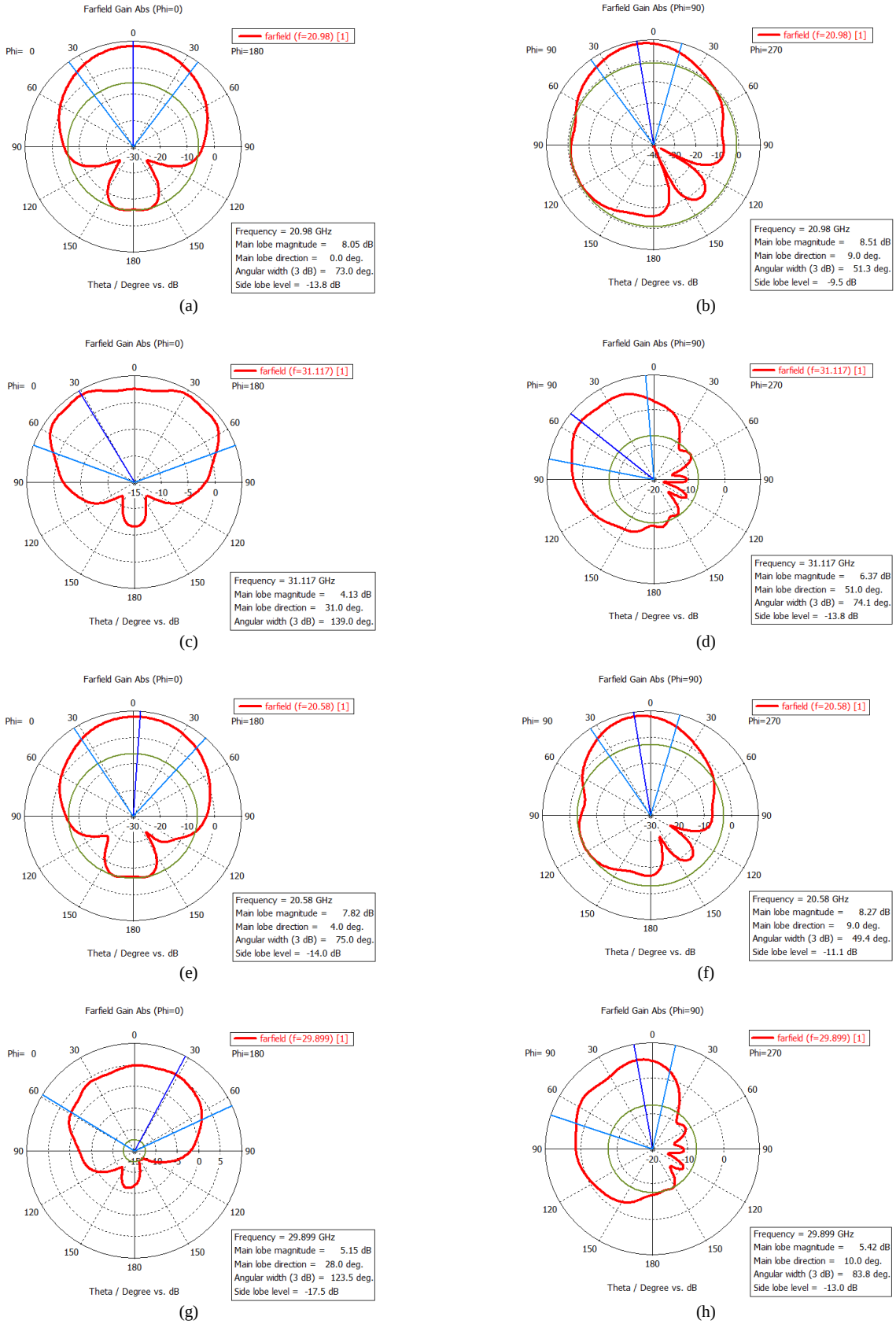

Fig. 8. Simulated Farfield 2D Polar radiation patterns (a): E-plane at 20.98 GHz, (b): H-plane at 20.98 GHz, (c): E-plane at 31.117 GHz, (d): H-plane at 31.117 GHz, (e): E-plane at 20.58 GHz, (f): H-plane at 20.58 GHz, (g): E-plane at 29.899 GHz, (h): H-plane at 29.899 GHz

Fig. 8(a) shows that the main lobe magnitude is 8.05 dB, the direction of the main lobe is 0 °and the angular width (3 dB) is 73 °at 20.98 GHz frequency when phi=0 °where Fig. 8(b) exhibits that the magnitude of the main lobe is 8.51

dB, the direction of the main lobe is 9 ° and the angular width is 51.3 ° at 20.98 GHz frequency when phi=90 °. Fig. 8(c) exhibits that the main lobe magnitude is 4.13 dB, the direction of the main lobe is 31 °, and the angular width is 139 ° at 31.117 GHz frequency, while Fig. 8(d) shows that the magnitude of the main lobe is 6.37 dB, the direction of the main lobe is 51 °, and the angular width is 74.1 ° at 31.117 GHz frequency when phi=90 °.

The 2D polar radiation patterns of the 1st modified antenna (step 2) for E-plane and H-plane at 20.58 GHz and 29.899 GHz resonance frequencies are illustrated in Fig. 8(e) to Fig. 8(h), respectively. Fig. 8(e) shows that the magnitude of the main lobe is 7.82 dB, the direction of the main lobe is 4 °, and the angular width (3 dB) is 75 ° at the 20.58 GHz resonance frequency where the side lobe level is -14 dB. Also, Fig. 8(f) exhibits that the magnitude of the main lobe is 8.27 dB and the angular width is 49.4 ° at 20.58 GHz frequency when phi=90 °. When phi=0 °, the main lobe magnitude is 5.15 dB, the direction of the main lobe is 28 °, the angular width is 123.5 ° at 29.899 GHz frequency, and the side lobe level is -17.5 dB which is shown in Fig. 8(g), where Fig. 8(h) shows that the magnitude of the main lobe is 5.42 dB, the direction of the main lobe is 10 °. The angular width is 83.8 ° at the same resonance frequency when phi=90 °.

The polar radiation patterns of the 2nd modified antenna (step 3) for the E-plane and H-plane at 19.962 GHz and 29.72 GHz resonance frequencies are illustrated in Fig. 9(a) to Fig. 9(d). Fig. 9(a) shows that the magnitude of the main lobe is 7.69 dB, the direction of the main lobe is 4 °, and the angular width (3 dB) is 77 ° at the 19.962 GHz resonance frequency when phi=0 °. Also, Fig. 9(b) exhibits that the magnitude of the main lobe is 8.06 dB and the angular width is 50.2 ° at 19.962 GHz frequency (when phi=90 °). When phi=0 °, the main lobe magnitude is 5.58 dB, and the direction of the main lobe is 31 °. The angular width is 130.9 ° at 29.72 GHz frequency, which is shown in Fig. 9(c), where Fig. 9(d) shows that the magnitude of the main lobe is 5 dB, the direction of the main lobe is 2 °, and the angular width is 44.8 ° at the 29.72 GHz resonance frequency when phi=90 °.

The simulated Farfield (2D Polar) radiation patterns of the proposed design at 19.28 GHz and 28.07 GHz resonance frequencies are illustrated in Fig. 9(e) to Fig. 9(h). Fig. 9(e) exhibits the farfield (2D polar) radiation pattern for 19.28 GHz frequency in the elevation plane "E-plane" (XZ-plane, $\phi = 0$ °). From Fig. 9(e), we see that the main lobe magnitude is 7.25 dB, the direction of the main lobe is 0 °, and the angular width (3 dB) is 79.2 ° at 19.28 GHz frequency. Besides, the farfield radiation pattern for the 19.28 GHz frequency in the azimuth plane "H-plane" (XY-plane, ϕ =90 °) is depicted in Fig. 9(f) where the magnitude of the main lobe is 7.61 dB, the direction of the main lobe is 8 °, and the angular width (3 dB) is 49.6 °. Here, the value of the side lobe level at 19.28 GHz resonant frequency is -14.1 dB.

On the other hand, the farfield polar radiation pattern for the 28.07 GHz frequency in the "E-plane" is shown in Fig. 9(g), where the magnitude of the main lobe is 6.97 dB, the direction of the main lobe is 0 °, and the angular width (3 dB) is 85.3 °. In the case of "E-plane", the value of side lobe levels at 19.28 GHz and 28.07 GHz resonance frequencies are -13.8 dB and -12.9 dB, respectively. Also, Fig. 9(h) exhibits the farfield (2D polar) radiation pattern in the "H-plane" (ϕ = 90 °). At 28.07 resonance GHz frequency, the magnitude of the main lobe is 6.97 dB, the direction of the main lobe is 0 °, and the angular width (3 dB) is 34.4 ° where the value of the sidelobe level is -6.9 dB.

An antenna's farfield (radiating farfield region) is independent of the distance from the antenna where the effective radiation pattern is observed. The simulated radiation gain vs. frequency plot is shown in Fig. 10. The directivity of an antenna can be defined as the direction of maximum radiation by the antenna as it radiates more in a particular direction defined by the antenna's main lobe. The simulated directivity vs. frequency plot is shown in Fig. 11. It has been seen that the values of directivity of the proposed slotted star-shaped patch antenna at 19.28 GHz and 28.07 GHz resonance frequencies are 8.9279 dBi and 8.1554 dBi, respectively.

4.5 Radiation Efficiency

The Antenna radiation efficiency explains how much an antenna can effectively deliver its output with minimal loss in the transmission line. Fig. 12 shows the proposed slotted star-shaped patch antenna's simulated radiation efficiency vs. frequency graph. The proposed antenna shows the overall radiation efficiency is 73.586% and 76.178% at 19.28 GHz and 28.07 GHz frequencies, respectively.

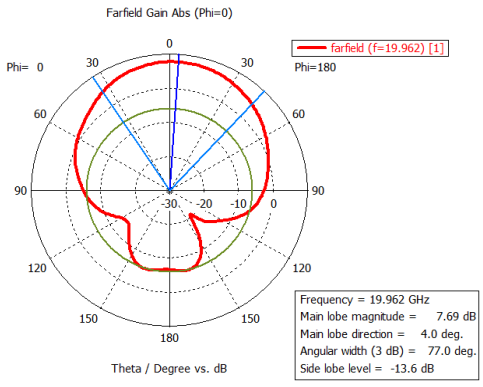

(a)

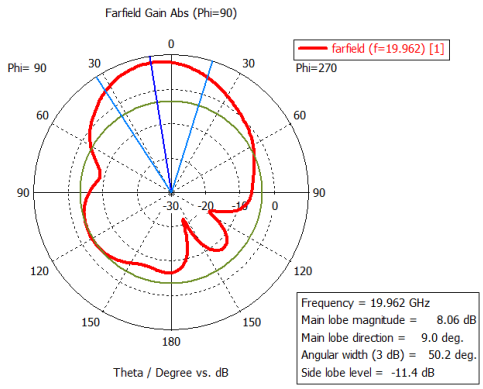

(b)

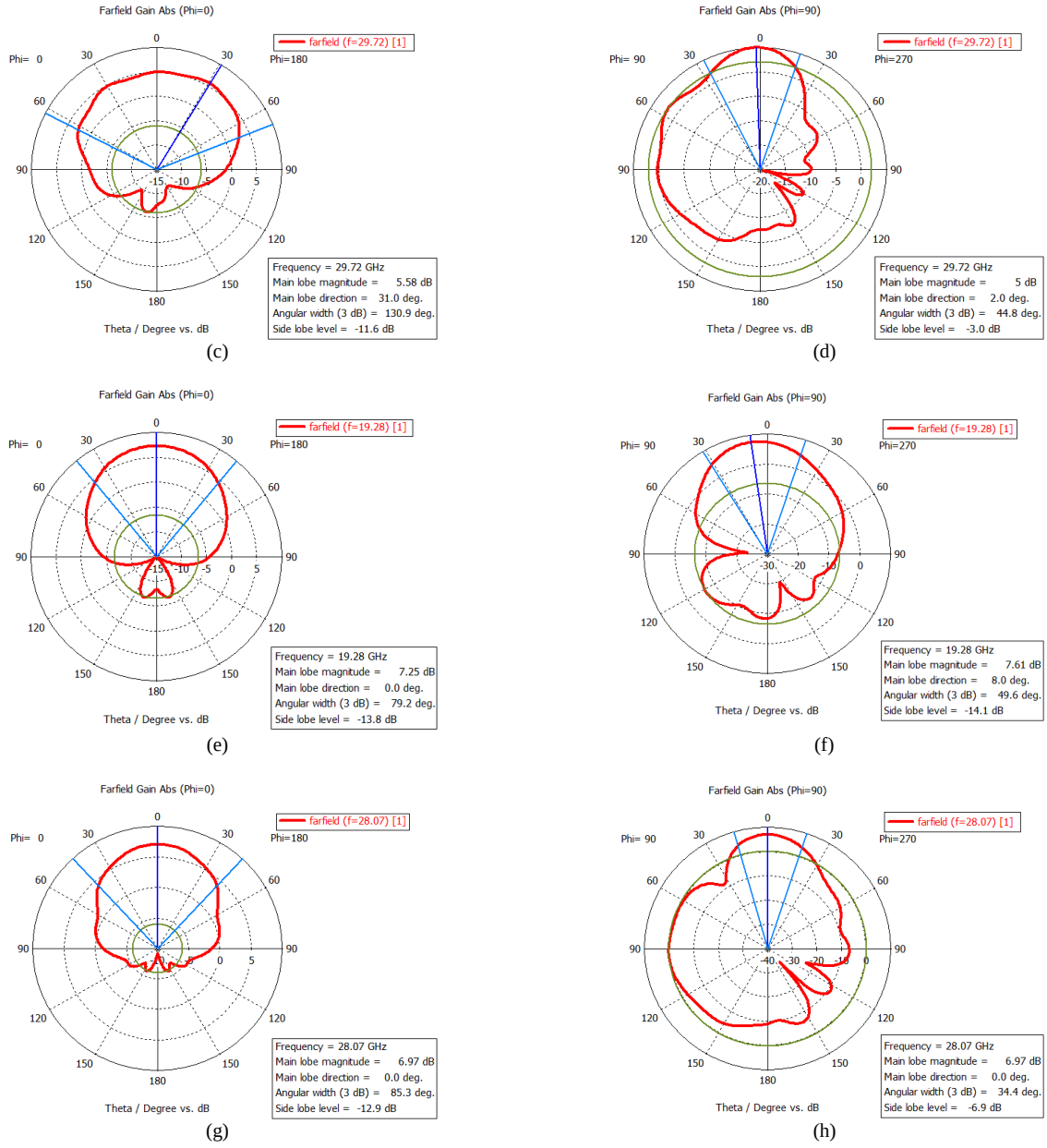

Fig. 9. Simulated Farfield 2D Polar radiation patterns (a): E-plane at 19.962 GHz, (b): H-plane at 19.962 GHz, (c): E-plane at 29.72 GHz, (d): H-plane at 29.72 GHz, (e): E-plane at 19.28 GHz, (f): H-plane at 19.28 GHz, (g): E-plane at 28.07 GHz, (h): H-plane at 28.07 GHz

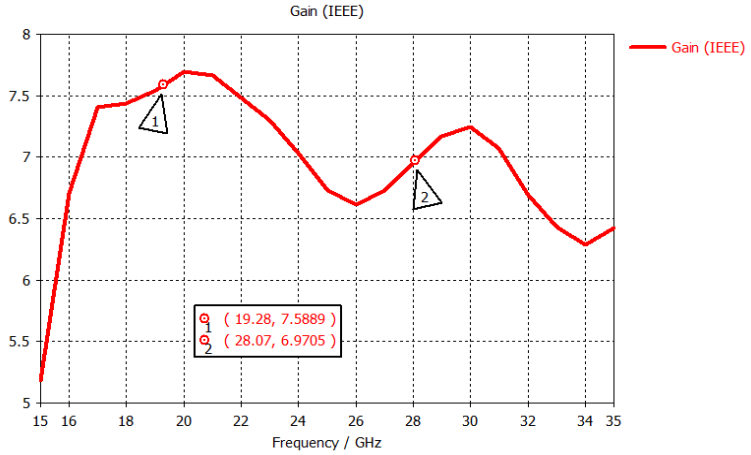

Fig. 10. Simulated radiation gain vs. frequency graph

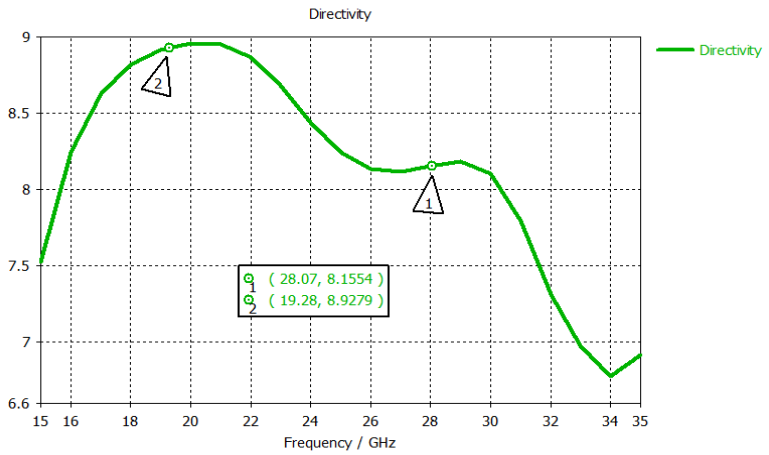

Fig. 11. Simulated directivity vs. frequency graph

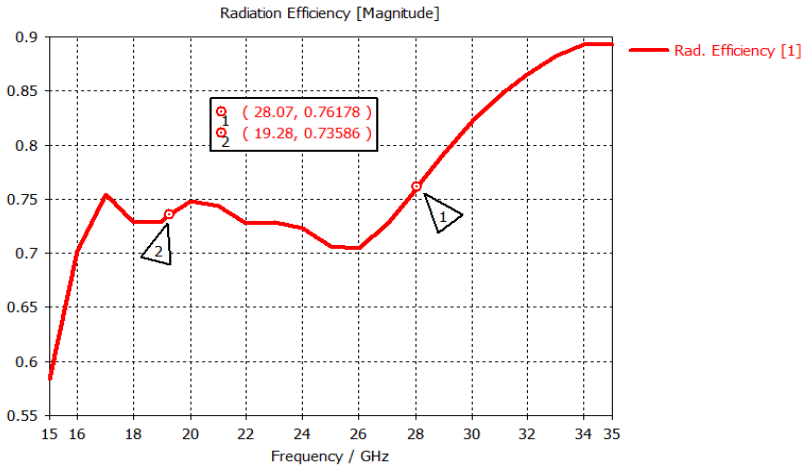

Fig. 12. Simulated radiation efficiency vs. frequency graph

5. Comparison with Related Work

A comparison with related works is shown in Table 2. The proposed slotted star-shaped patch antenna exhibits very good performance like wide bandwidth, high radiation gain, better radiation efficiency, and so on. It is demonstrated that the proposed design exhibits better performance than the reported work.

Table 2. Comparative Analysis.

Ref.	Values (mm^3)	Bandwidth (GHz)	Peak Gain (dB)
[1]	20×20×1.575	1.11 1.15	1.87 3.87
[10]	7.2×6.2×0.5	0.989 0.222	6.4 5.4
[12]	7.6×4.9×0.127	Not reported	5.541 4.527
[14]	10×10×0.5	2.00	5.45
[15]	25×20×1.6	1.90 1.01	3.20 3.99
[17]	65×56×1.6	0.100 0.230	7.03 7.77
[19]	24.5×24.5×0.38	0.338 0.733	5.59 6.10
Proposed Work	15×14×1.6	1.011 2.161	7.596 6.972

6. Conclusions

This paper proposes a slotted star-shaped dual-band patch antenna for the integrated services of satellite communication and 5G mobile services. Design and simulation have been carried out using the computer simulation technology microwave studio (CST-MWS) software. The proposed slotted star-shaped dual-band patch antenna exhibits very good performance with higher data rates, relatively high efficiency, high radiation gain, and so on. The proposed antenna resonates at 19.28 GHz and 28.07 GHz frequencies with a radiation gain of 7.596 dB and 6.972 dB, respectively, whereas the overall radiation efficiencies are 73.586% and 76.178%, respectively.

Acknowledgment

The authors thank the reviewers for their valuable comments, suggestions, and questions that significantly improved the article.

References

[1] M. M. Islam, et el., "Design of a microstrip antenna on duroid 5870 substrate material for ku and k-band applications." Technical Gazette 22, no. 1 (2015): 71-77.
[2] K. Ullah, Kifayat, et el., "Design and Analysis of a Compact Dual-Band Patch Antenna for 5G mmW Application." In 2020 14th International Conference on Open Source Systems and Technologies (ICOSST), pp. 1-5. IEEE, 2020.
[3] T. R. Raddo, et el., "Transition technologies towards 6G networks." EURASIP Journal on Wireless Communications and Networking 2021, no. 1 (2021): 1-22.
[4] M. A. M. Albreem, et el., "5G wireless communication systems: Vision and challenges." In 2015 International Conference on Computer, Communications, and Control Technology (I4CT), pp. 493-497. IEEE, 2015.
[5] N. Panwar, et el., "A survey on 5G: The next generation of mobile communication." Physical Communication 18 (2016): 64-84.
[6] T. S. Rappaport, et el., "Millimeter wave mobile communications for 5G cellular: It will work!." IEEE access 1 (2013): 335-349.
[7] Z. Bojkovic, et el., "A technology vision of the fifth generation (5g) wireless mobile networks." In International Conference on Emerging Trends in Electrical, Electronic and Communications Engineering, pp. 25-43. Springer, Cham, 2016.
[8] M. N. Hossain, et el., "Multiband Slotted Crescent-shaped Patch Antenna for K-band Satellite and mmWave Communications." IEIE Transactions on Smart Processing & Computing 11, no. 3 (2022): 213-221.
[9] C. Seker, et el., "A review of millimeter wave communication for 5G." In 2018 2nd International Symposium on Multidisciplinary Studies and Innovative Technologies (ISMSIT), pp. 1-5. IEEE, 2018.
[10] A. Khan, et el., "Compact Rectangle Patch Dual Band High Gain Antenna for mm-Wave 5G Applications." In 2021 Sixth International Conference on Wireless Communications, Signal Processing and Networking (WiSPNET), pp. 188-191. IEEE, 2021.
[11] C. K. Ali, et el., "Dual-band millimeter-wave microstrip patch array antenna for 5G smartphones." In 2019 International Conference on Advanced Science and Engineering (ICOASE), pp. 181-185. IEEE, 2019.
[12] N. N. Daud, et el., "A dual band antenna design for future millimeter wave wireless communication at 24.25 GHz and 38 GHz." In 2017 IEEE 13th International Colloquium on Signal Processing & its Applications (CSPA), pp. 254-257. IEEE, 2017.
[13] W. A. Awan, et el., "Patch antenna with improved performance using DGS for 28GHz applications." In 2019 international conference on wireless technologies, embedded and intelligent systems (WITS), pp. 1-4. IEEE, 2019. Article (CrossRef Link)
[14] D. E. Hadri, et el., "The study of a 5G antenna with encoche and Defected Ground Structure (DGS) using the Iterative Method." In 2019 International Conference on Wireless Technologies, Embedded and Intelligent Systems (WITS), pp. 1-6. IEEE, 2019.
[15] F. Kaburcuk, et el., "A Dual-Band and Low-Cost Microstrip Patch Antenna for 5G Mobile Communications." The Applied Computational Electromagnetics Society Journal (ACES) (2021): 824-829.
[16] M. E. Ouahabi, et el., "A miniaturized dual-band MIMO antenna with low mutual coupling for wireless applications." Progress In Electromagnetics Research C 93 (2019): 93-101.
[17] M. F. Nakmouche, et el., "Dal band SIW patch antenna based on H-slotted DGS for Ku band application." In 2020 7th International Conference on Electrical and Electronics Engineering (ICEEE), pp. 194-197. IEEE, 2020.
[18] M. T. Islam, et el., "Compact dual band microstrip antenna for Ku-band application." Information Technology Journal 9, no. 2 (2010): 354-358.
[19] M. F. Nakmouche, et el., "Low profile dual band H-slotted DGS based antenna design using ANN for K/Ku band applications." In 2021 8th International Conference on Electrical and Electronics Engineering (ICEEE), pp. 283-286. IEEE, 2021.
[20] A. Sayed, et el., "Design of a compact dual band microstrip antenna for ku-band applications." International Journal of Computer Applications 115, no. 13 (2015).
[21] M. E. Jourmi, et el., "Design and simulation of UWB microstrip patch antenna for Ku/K bands applications." International Journal of Electrical and Computer Engineering 9, no. 6 (2019): 4845.
[22] R. Ahmed, et el., "E-shaped microstrip patch antenna for Ku band." International Journal of Computer Applications 80, no. 6 (2013).
[23] R. H. Thaher, et el., "Design of dual band elliptical microstrip antenna for satellite communication." In IOP Conference Series: Materials Science and Engineering, vol. 928, no. 2, p. 022066. IOP Publishing, 2020.
[24] M. J. Rana, et el., "Numerical study of a loaded U-antenna for 3.5 GHz mobile WiMAX and 7.5 GHz military satellite communication applications." In 16th Int'l Conf. Computer and Information Technology, pp. 283-286. IEEE, 2014.

[25] M. M. Rahman, et el., "Compact Multiple Wideband Slotted Circular Patch Antenna for Satellite and Millimeter-Wave Communications." In 2021 International Conference on Information and Communication Technology Convergence (ICTC), pp. 233-236. IEEE, 2021.
[26] M. Zahid, et el., "Ultra wideband antenna for Future 5G." In 2020 IEEE conference of Russian young researchers in electrical and electronic engineering (EIConRus), pp. 2280-2283. IEEE, 2020.
[27] M. M. Rahman, et el., "A Compact Slotted Patch Antenna Design for Multiband Applications." In 2021 IEEE Asia Pacific Conference on Wireless and Mobile (APWiMob), pp. 147-150. IEEE, 2021.
[28] M. Samsuzzaman, et el., "Design of a compact new shaped microstrip patch antenna for satellite application." Advances in Natural and Applied Sciences 6, no. 6 (2012): 898-903.
[29] D. E. Hadri, et el., "A Compact Triple Band Antenna for Military Satellite Communication, Radar and Fifth Generation Applications." Advanced Electromagnetics 9, no. 3 (2020): 66-73.
[30] S. Pandey, et el., "Design and analysis of circular shape microstrip patch antenna for C-band applications." International Journal of Advanced Research in Computer Science & Technology 4, no. 2 (2016): 169-171.
[31] M. A. Nasr, et al., "Design of star-shaped microstrip patch antenna for ultra wideband (UWB) applications." International Journal of Wireless & Mobile Networks 5, no. 4 (2013): 65-73.

Authors' Profiles

Md. Najmul Hossain was born in Rajshahi, the People's Republic of Bangladesh in 1984. He is currently working as an Associate Professor in the Department of Electrical, Electronic and Communication Engineering, Pabna University of Science and Technology, Pabna, Bangladesh. He received his B.Sc. and M.Sc. degrees in Applied Physics and Electronic Engineering (Presently named as, Electrical and Electronic Engineering) from the University of Rajshahi, Rajshahi, Bangladesh, in 2007 and 2008, respectively. In 2010, he was also awarded a Gold Medal for his excellent academic performance. In 2020, he received his Ph.D. in Advanced Wireless Communication Systems at the Graduate School of Science and Engineering, Saitama University, Saitama, Japan. He serves as an Editor of the Journal of Engineering Advancements (JEA). Also, he has served as a reviewer of several SCIE/Scopus journals and international conferences. His current research interests include smart antenna design, advanced wireless communication systems, and corresponding signal processing, especially for OFDM, OTFS, MIMO, and future-generation wireless communication networks.

Al Amin Islam received his B.Sc. degree in the Department of Electronic and Telecommunication Engineering (Presently named as, Electrical, Electronic and Communication Engineering), Pabna University of Science and Technology, Pabna, Bangladesh. His research interests are Antenna Design, Wave Propagation, and Wireless Communication.

Jungpil Shin (Senior Member, IEEE) received a B.Sc. in Computer Science and Statistics and an M.Sc. in Computer Science from Pusan National University, Korea, in 1990 and 1994, respectively. He received his Ph.D. in computer science and communication engineering from Kyushu University, Japan, in 1999, under a scholarship from the Japanese Government (MEXT). He was an Associate Professor, a Senior Associate Professor, and a Full Professor at the School of Computer Science and Engineering, the University of Aizu, Japan, in 1999, 2004, and 2019, respectively. He has co-authored more than 250 published papers for widely cited journals and conferences. His research interests include pattern recognition, image processing, computer vision, machine learning, human-computer interaction, non-touch interfaces, human gesture recognition, automatic control, Parkinson's disease diagnosis, ADHD diagnosis, user authentication, machine intelligence, as well as handwriting analysis, recognition, and synthesis. He is a member of ACM, IEICE, IPSJ, KISS, and KIPS. He has served as program chair and as a program committee member for numerous international conferences. He serves as an Editor of IEEE journals and for MDPI Sensors. Also, he serves as a reviewer for several major IEEE and SCI journals.

Md. Abdur Rahim received his Ph.D. in 2020 in Computer Science and Engineering from the University of Aizu, Japan. He is an Associate Professor and Chairman of the Department of Computer Science and Engineering, Pabna University of Science and Technology, Pabna, Bangladesh. He received his Bachelor of Science (Honours) and Master of Science in Computer Science and Engineering from the University of Rajshahi, Bangladesh, in 2008 and 2009. His current research interests include human-computer interaction, pattern recognition, computer vision and image processing, human recognition, and machine intelligence. He has been a reviewer for several major SCI/SCIE journals and a Technical Program Committee member for many conferences.

Md. Humaun Kabir received his B.Sc. Engineering and M.Sc. Engineering degree in Applied Physics and Electronic Engineering (presently named as, Electrical and Electronic Engineering) from the University of Rajshahi, Bangladesh. Currently, he is working as an Assistant Professor in the Department of Computer Science and Engineering, Bangamata Sheikh Fojilatunnesa Mujib Science & Technology University, Jamalpu-2012, Bangladesh. His research interests include Next Generation Wireless Communications, Biomedical Signal Processing, and Brain-computer interfacing.

How to cite this paper: Md. Najmul Hossain, Al Amin Islam, Jungpil Shin, Md. Abdur Rahim, Md. Humaun Kabir, "Performance Evaluation of Slotted Star-Shaped Dual-band Patch Antenna for Satellite Communication and 5G Services", International Journal of Wireless and Microwave Technologies(IJWMT), Vol.13, No.3, pp. 49-63, 2023. DOI:10.5815/ijwmt.2023.03.05